Opposite outcomes of coinfection at individual and population scales

Gorsich, Erin E.; Etienne, Rampal S.; Medlock, Jan; Beechler, Brianna R.; Spaan, Johannie M.; Spaan, Robert S.; Ezenwa, Vanessa O.; Jolles, Anna E.

Published in:
Proceedings of the National Academy of Sciences of the United States of America

DOI:
10.1073/pnas.1801095115

Publication date:
2018

Opposite outcomes of coinfection at individual and population scales

Erin E. Gorsich[a,b,c,1], Rampal S. Etienne[d], Jan Medlock[a], Brianna R. Beechler[a], Johannie M. Spaan[b], Robert S. Spaan[e], Vanessa O. Ezenwa[f,g], and Anna E. Jolles[a]

[a]Department of Biomedical Sciences, Oregon State University, Corvallis, OR 97331; [b]Department of Integrative Biology, Oregon State University, Corvallis, OR 97331; [c]Department of Biology, Colorado State University, Fort Collins, CO 80523; [d]Groningen Institute for Evolutionary Life Sciences, University of Groningen, 9700 CC Groningen, The Netherlands; [e]Department of Fisheries and Wildlife, Oregon State University, Corvallis, OR 97331; [f]Odum School of Ecology, College of Veterinary Medicine, University of Georgia, Athens, GA 30602; and [g]Department of Infectious Diseases, College of Veterinary Medicine, University of Georgia, Athens, GA 30602

Edited by Nils Chr. Stenseth, University of Oslo, Oslo, Norway, and approved June 8, 2018 (received for review January 20, 2018)

Coinfecting parasites and pathogens remain a leading challenge for global public health due to their consequences for individual-level infection risk and disease progression. However, a clear understanding of the population-level consequences of coinfection is lacking. Here, we constructed a model that includes three individual-level effects of coinfection: mortality, fecundity, and transmission. We used the model to investigate how these individual-level consequences of coinfection scale up to produce population-level infection patterns. To parameterize this model, we conducted a 4-y cohort study in African buffalo to estimate the individual-level effects of coinfection with two bacterial pathogens, bovine tuberculosis (bTB) and brucellosis, across a range of demographic and environmental contexts. At the individual level, our empirical results identified bTB as a risk factor for acquiring brucellosis, but we found no association between brucellosis and the risk of acquiring bTB. Both infections were associated with reductions in survival and neither infection was associated with reductions in fecundity. The model reproduced coinfection patterns in the data and predicted opposite impacts of coinfection at individual and population scales: Whereas bTB facilitated brucellosis infection at the individual level, our model predicted the presence of brucellosis to have a strong negative impact on bTB at the population level. In modeled populations where brucellosis was present, the endemic prevalence and basic reproduction number (R_0) of bTB were lower than in populations without brucellosis. Therefore, these results provide a data-driven example of competition between coinfecting pathogens that occurs when one pathogen facilitates secondary infections at the individual level.

African buffalo | brucellosis | tuberculosis | coinfection | competition

Over one-sixth of the global human population is estimated to be affected by coinfection [concurrent infection by multiple pathogens (1)]. Their ubiquity includes over 270 pathogen taxa and many important chronic infections, such as hepatitis-C, HIV, TB, and schistosomiasis (1–3). Mounting evidence suggests that coinfecting pathogens can interact within the host to influence the individual-level clinical outcomes of infection (4, 5). These interactions may also influence the spread of infections at the population level (6, 7). Understanding the effects of coinfection at both levels may, therefore, be fundamental to the success of integrated treatment and control programs that target multiple infections (8, 9).

One challenge to predicting the epidemiological consequences of coinfection is that the mechanisms of parasite interaction—and their resulting changes to susceptibility or disease progression—occur within the host, while patterns relevant for disease control occur within a population (10). Bridging these individual and population scales requires synthesizing multiple, individual-level processes across natural demographic and environmental variation. For example, in an ecosystem with more than one pathogen, infection with one pathogen may be one of the best predictors of individual-level risk for infection with a second pathogen (11, 12), resulting in increased or decreased transmission. Coinfecting pathogens may also moderate the individual-level survival and fecundity costs of infection (4, 13). However, the population-level consequences of coinfection are influenced by the net effects of these potentially nonlinear individual-level processes (14, 15).

At the population level, theoretical studies have highlighted the range of dynamics generated by coinfecting pathogens (6, 16, 17). Even for unrelated pathogens, coinfection can dramatically modify infection dynamics through ecological mechanisms such as convalescence and disease-induced mortality (15, 18–21). This theoretical work builds on a detailed database of childhood infections, thereby providing a data-driven understanding of coinfection dynamics for acute, immunizing infections. In contrast, data and theory on the effects of coinfection with long-lasting infections are limited (but see ref. 22). Chronic coinfections are of particular interest in this context because they are responsible for the majority of coinfections (1) and have the potential to dramatically alter infection patterns (14). Their protracted presence in the host brings increased complexity to pathogen interactions, challenging model development and

Significance

Infection with multiple parasite species is common and the majority of coinfections involve at least one long-lasting infection. Our data-driven model of chronic coinfection dynamics shows that accurate prediction at the population level requires quantifying both the individual-level transmission and mortality consequences of coinfection. The infections characterized in this study compete at the population level. When one pathogen facilitates both the transmission and progression of the second pathogen, the prevalence of the first pathogen is reduced. This mechanism of competition is unique compared with previously described mechanisms and occurs without cross-immunity, resource competition within the host, or convalescence. We recommend assessing the generality of this mechanism, which could have important consequences for other chronic, immunosuppressive pathogens such as HIV or TB.

Author contributions: E.E.G., R.S.E., J.M., V.O.E., and A.E.J. designed research; E.E.G., R.S.E., and J.M. performed research; E.E.G., R.S.E., J.M., B.R.B., V.O.E., and A.E.J. analyzed data; E.E.G., R.S.E., J.M., B.R.B., J.M.S., R.S.S., V.O.E., and A.E.J. wrote the paper; and E.E.G., B.R.B., J.M.S., R.S.S., V.O.E., and A.E.J. collected the data.

The authors declare no conflict of interest.

This article is a PNAS Direct Submission.

[1]To whom correspondence should be addressed. Email: eringorsich@gmail.com.

This article contains supporting information online at www.pnas.org/lookup/suppl/doi:10.1073/pnas.1801095115/-/DCSupplemental.

Published online July 2, 2018.

evaluation. Detailed longitudinal sampling or experimental studies are required to unravel their precise mechanisms and potentially asymmetric outcomes of interaction (22). Few datasets simultaneously estimate the individual-level transmission, survival, and fecundity consequences of coinfection. To address this gap, we provide a data-driven investigation of coinfection dynamics for chronic pathogens.

We focus our research on two chronic bacterial infections, bovine tuberculosis (bTB) and brucellosis, in a wild population of African buffalo (*Syncerus caffer*) to ask: How do the individual-level consequences of coinfection scale up to produce population-level infection patterns? This system allows us to simultaneously monitor both individual and population levels of the infection process (4, 7) in a natural reservoir host (23, 24). Furthermore, bTB and brucellosis have well-characterized and asymmetric effects on the within-host environment. bTB is a directly transmitted, life-long respiratory infection that causes dramatic and systemic changes to host immunity (25). African buffalo infected with bTB have reduced innate immune function and increased inflammatory responses (4). Conversely, brucellosis is a persistent infection of the reproductive system. It persists within phagocytic cells (26), and although infection also invokes an inflammatory response, it is less severe and more localized compared to the immune response to bTB (27). These differences and our ability to observe the natural history of both infections make bTB and brucellosis an ideal system to explore disease dynamics across scales.

Our approach combines a mathematical model of the coinfection dynamics of bTB and brucellosis and a 4-y cohort study of 151 buffalo (Fig. 1). For this model, all parameters describing the consequence of coinfection were estimated from field data; they include the individual-level, per capita consequences of coinfection on mortality, fecundity, and infection risk. We quantified these parameters by tracking the individual infection profiles of each buffalo, which were monitored at approximately 6-mo intervals and resulted in over 4,386 animal months of observation time from two capture sites. We show that the model accurately reproduces observed coinfection patterns and use the model to predict the reciprocal effects of brucellosis and bTB on each other's dynamics at the population level. In addition, we assess the relative importance of each individual-level process on coinfection dynamics.

Results

Individual-Level Consequences of Coinfection: Model Parameterization. bTB and brucellosis were associated with multiplicative increases in mortality (Fig. 2*A* and *SI Appendix*, section 1, Table S1). Approximate annual mortality rates in the data were 0.056 (10 mortalities/175.75 animal years) in uninfected buffalo, 0.108 (6 mortalities/55.5 animal years) in buffalo with bTB alone, 0.144 in buffalo with brucellosis alone (13 mortalities/90.5 animal years), and 0.21 in coinfected buffalo (9 mortalities/43.8 animal years). After accounting for environmental and demographic covariates with a Cox proportional hazards regression model, bTB was associated with a 2.82 (95% CI 1.43–5.58)-fold increase in mortality, and infection with brucellosis was associated with a 3.02 (95% CI 1.52–6.01)-fold increase in mortality compared with uninfected buffalo. Coinfected buffalo were associated with an 8.58 (95% CI 3.20–22.71)-fold increase in mortality compared with uninfected buffalo (Fig. 2*A*). Mortality rates were also influenced by buffalo age and capture site, but the effect of coinfection remained consistent across all ages and in both sites. Neither infection was associated with reductions in fecundity (described in detail in *SI Appendix*, section 1, Fig. S1). Uninfected buffalo were observed with a calf 68% (11/16) of the time compared with 37% (6/16), 29% (7/24), and 57% (4/7) in bTB-positive, brucellosis-positive, and coinfected adult buffalo.

The consequences of coinfection on infection risk were asymmetric, with bTB facilitating brucellosis infection but not vice versa (Fig. 2*B* and *SI Appendix*, section 1, Table S2). Approximate brucellosis incidence rates were 0.05 (18 infections/340 animal years) in uninfected buffalo compared with 0.08 (8 infections/104 animal years) in buffalo with bTB (*SI Appendix*, section 1, Fig. S2). Approximate bTB incidence rates were 0.08 (27 infection/340 animal years) in uninfected buffalo and 0.07 (9 infections/138 animal years) in buffalo with brucellosis. After accounting for demographic covariates in a Cox proportional hazards regression model, brucellosis infection risk

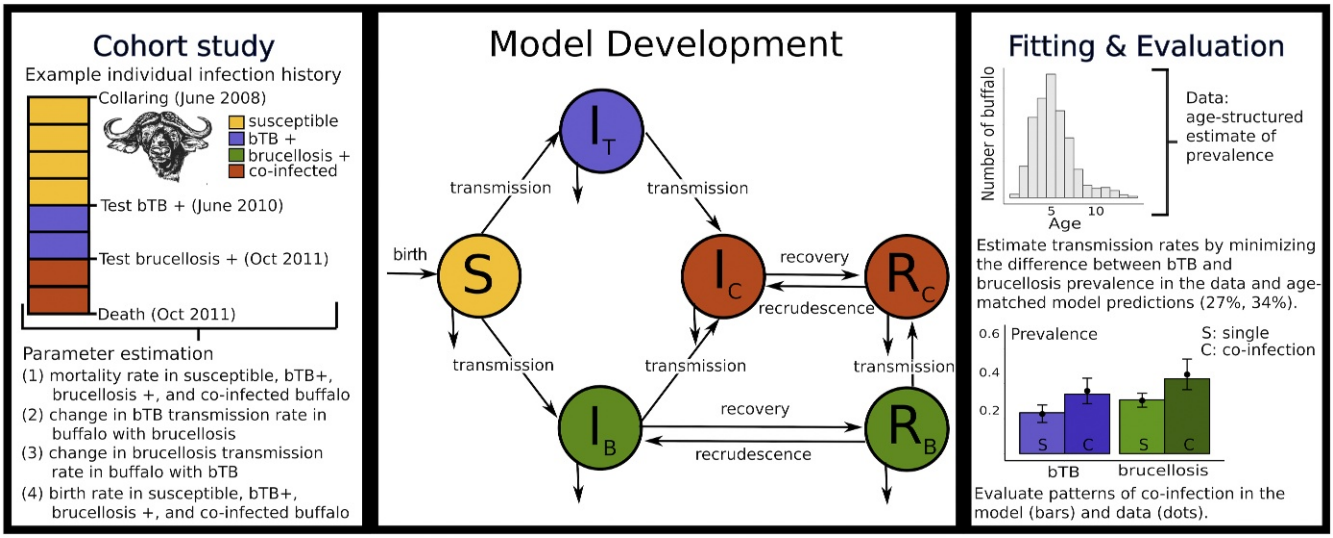

Fig. 1. Conceptual diagram of the data, model, and evaluation. (*Center*) A schematic representation of the disease model defined in *SI Appendix*, section 2. Hosts are represented as susceptible (*S*), infected with bTB only (I_T), infected with brucellosis only (I_B), coinfected with both infections (I_C), persistently infected with brucellosis only but no longer infectious (R_B), and persistently infected with brucellosis but no longer infectious and coinfected with bTB (R_C). (*Left*) A detailed cohort study informs model parameterization by quantifying the mortality, transmission, and fecundity consequences of coinfection (*Right*) as well as the transmission parameters for both infections. (*Right*) The prevalence plot illustrates that the model accurately reproduces coinfection patterns in the data. The bars represent the proportion of single (S) and coinfected (C) individuals in the model results and the solid circles represent the data.

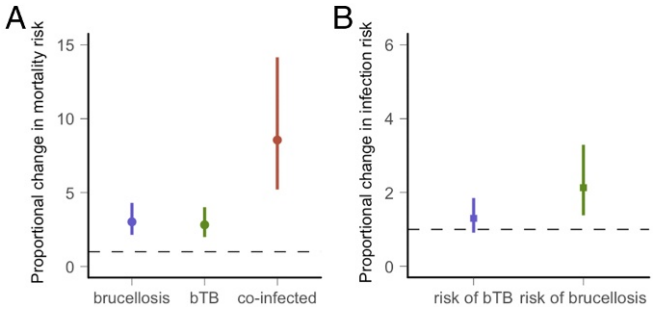

Fig. 2. Parameter estimation based on Cox proportional hazards analyses of the cohort study. (*A*) The predicted median and SE for the proportional change in mortality when buffalo are infected with brucellosis or bTB or coinfected relative to uninfected buffalo. (*B*) The predicted estimates for the proportional change in infection risk when buffalo are infected with another pathogen relative to the risk in uninfected buffalo. The dashed line indicates no change in risk.

was 2.09 (95% CI 0.89–4.91) times higher in buffalo with bTB compared with susceptible buffalo. bTB infection risk was similar in uninfected buffalo and buffalo with brucellosis. The association between prior infection with bTB and brucellosis infection risk varied by capture site, with the association between bTB and brucellosis infection risk ranging from no change at one site to a 4.32 (95% CI 1.51–12.37)-fold higher risk at the other site (interaction term for bTB × site: P value = 0.045 and *SI Appendix*, section 1, Table S2). The regression model also identified an association between brucellosis infection risk and buffalo age. Early reproductive-aged buffalo had an increased infection risk.

Population-Level Consequences of Coinfection: Basic Reproduction Number and Prevalence. We built a disease dynamic model to translate the individual-level effects quantified above into predicted population-level effects of coinfection (Fig. 1 and *SI Appendix*, section 2). Our disease model parameterization, therefore, represents increased risk of acquiring brucellosis in early reproductive-aged buffalo and the average effect of bTB on brucellosis infection risk across sites. For example, to represent increased brucellosis infection risk in buffalo with bTB, we specify a higher transmission rate for buffalo with bTB compared with the transmission rate for uninfected buffalo. *SI Appendix*, section 2, Tables S3 and S4 provides additional detail on model parameterization and defines how the consequences of coinfection quantified in our data analyses were translated into model parameters.

We estimated parameter values for the transmission rate of bTB and brucellosis by minimizing the sum of squared errors between the overall bTB and brucellosis infection prevalence in our data and in an age-matched sample from the model after it had reached equilibrium (*SI Appendix*, section 2, Fig. S4). bTB prevalence in the data was 27% and brucellosis prevalence was 34%. The resulting transmission rate parameters (brucellosis transmission rate in uninfected buffalo, 0.576; brucellosis transmission rate in buffalo with bTB, 1.20; bTB transmission rate in uninfected buffalo and in buffalo with brucellosis, 0.0013; *SI Appendix*, section 2, Table S4) accurately predict the positive association between bTB and brucellosis observed in the data (Fig. 1, *Right*, *Inset* bar plot) and allow us to predict the prevalence and basic reproduction number in modeled populations with and without coinfection. The basic reproduction number, R_0^i (i = T, B for infection with bTB or brucellosis) is defined as the average number of secondary cases generated by a single infection in a susceptible population.

In modeled populations, the presence of brucellosis infection results in large reductions in R_0^T, with a predicted R_0^T = 3.4 in populations where brucellosis is absent and R_0^T = 1.5 in populations where brucellosis is present. The predicted bTB prevalence is also lower in populations where both pathogens occur, with a bTB prevalence of 65.8% in populations where brucellosis is absent compared with 27.9% when both pathogens co-occur. Conversely, the presence or absence of bTB has only minor effects on the R_0^B and brucellosis prevalence. To represent uncertainty in the individual-level consequences of coinfection, we used Monte Carlo sampling of the parameters quantified in our statistical analyses (Fig. 2 and *SI Appendix*, section 2, Table S5). Fig. 3 displays the effect of coinfection when uncertainty in input parameters is considered. In this range of parameter values (parameter space), 96% of model trajectories predict a lower bTB prevalence in populations with brucellosis than in populations without brucellosis. In the remaining 4%, brucellosis did not persist in populations with or without coinfection due to high mortality rates and low facilitation rates (*SI Appendix*, section 2, Fig. S5).

To generalize these results, we compared infection prevalence in modeled populations with and without coinfection over a range of parameter values. We manipulated the infection

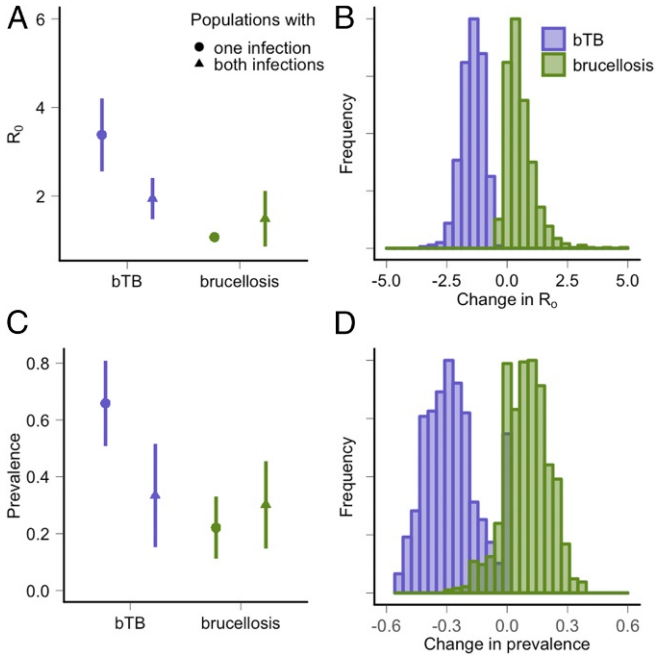

Fig. 3. Model predictions of the reciprocal consequences of coinfection in populations where one or both pathogens occur. Purple represents the model predictions of (*A* and *B*) R_0 and (*C* and *D*) prevalence for bTB; green represents predictions of R_0 and prevalence for brucellosis. For example, the purple circles and lines represent the median and SE prediction for bTB in populations where only bTB occurs. The purple triangles represent the prediction for bTB in populations where both pathogens are present. We used Monte Carlo sampling to quantify the uncertainty in model outcomes due to uncertainty in the parameters describing the individual-level consequences of coinfection (Fig. 2 and *SI Appendix*, section 2). (*A*) The estimated R_0 for bTB was lower in populations where brucellosis co-occurs while the estimated R_0 for brucellosis was similar in populations with and without bTB. (*B*) Histograms showing the difference in R_0 in populations where one or both pathogens are present. For each parameter set, change is calculated as the predicted value of bTB prevalence (purple) or brucellosis prevalence (green) in populations with coinfection subtracted by the predicted value in populations with a single pathogen. (*C*) The estimated prevalence of bTB was lower in populations where brucellosis co-occurs, while the estimated prevalence of brucellosis was similar in populations with and without bTB. (*D*) Histograms showing the difference in prevalence in populations where one or both pathogens are present.

ECOLOGY

risk (e.g., transmission rate) and mortality consequences of coinfection to explore other environmental contexts where the individual-level effects of coinfection may be reduced or exacerbated (Fig. 4). For two pathogens, A and B, the results suggest that pathogen A will have a negative effect on the prevalence of pathogen B if coinfected individuals have elevated mortality and infection with pathogen A results in reduced or similar susceptibility to pathogen B. In contrast, pathogen A is predicted to have a positive effect on the prevalence of pathogen B if infection results in an increased transmission rate for pathogen B and minimal changes in mortality with coinfection. When coinfection is associated with changes in both the transmission and mortality rates, the population-level consequences of coinfection depend on the type of pathogen considered. Specifically, bTB prevalence is lower in modeled populations with brucellosis for most parameter values while the effect of bTB on brucellosis is more variable.

At the parameter values quantified in our empirical dataset, these results illustrate that the lower bTB prevalence in populations where brucellosis co-occurs is driven by two mechanisms: (*i*) bTB is associated with increases in the transmission rate of brucellosis but not vice versa and (*ii*) coinfection is associated with increased mortality. As a result, at the individual level, buffalo infected with bTB are more likely to become infected with brucellosis and die than their uninfected counterparts. The resulting reductions in infection duration mean that the presence of brucellosis is predicted to reduce bTB prevalence at the population level. These results are robust to several important changes in the model structure, including alternative forms of density dependence, a range of values for the model parameters (*SI Appendix*, section 2, Figs. S6–S8), and density- vs. frequency-dependent transmission terms. Model dynamics in all formulations are qualitatively similar, although there is some variation in overall magnitude of change with coinfection.

Discussion

Our study provides a mechanistic understanding of how chronic coinfections mediate each other's dynamics. Model dynamics show that a pathogen can increase or decrease the prevalence of a second pathogen, depending on the net effect of infection on the transmission rate and infection duration of the second pathogen, the latter via mortality. When infection with one pathogen modifies only the transmission or only the mortality rate of the second pathogen, the prevalence of the second pathogen predictively increases or decreases (Fig. 4 and *SI Appendix*, section 2, Figs. S7 and S8). Previous work has quantified the disease-dynamic consequences of changes in transmission through a range of mechanisms: cross-immunity, antibody-mediated enhancement, immunosuppression, and convalescence (16, 20, 28, 29). Here, we show that transmission and mortality should be considered concurrently, following theoretical predictions (14, 22, 30). When pathogens modify both processes, nonlinear responses mediated through the coinfecting pathogen can have a large impact on population-level disease dynamics.

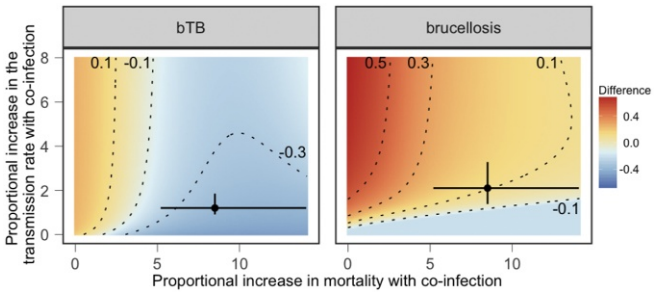

Fig. 4. The difference between predicted (*Left*) bTB or (*Right*) brucellosis prevalence values in populations where one or both pathogens are present. The axes represent a range of transmission rate and mortality consequences of coinfection. Proportional increases in mortality represent the mortality rate in coinfected individuals divided by the rate in susceptible individuals. Proportional increases in the transmission rate represent the transmission rate of the focal pathogen in individuals infected with the second pathogen divided by the transmission rate of the focal pathogen for susceptible individuals. Red indicates that the prevalence of the focal pathogen is higher in populations where the second pathogen is present; blue indicates that the prevalence of the focal pathogen is lower in populations where the second pathogen is present; yellow indicates no change. Contour lines indicate changes in prevalence by 20%. Circles and error bars indicate median and SE parameter values estimated in the data.

By exploring the coinfection dynamics of bTB and brucellosis, we also provide a data-driven example of competition between pathogens in a natural population. Here, the mechanism driving competition is different from previously described examples that focus on cross-immunity (29), resource competition within the host (31, 32), or ecological competition by convalescence (20, 21). The mechanism of parasite interaction in these examples occurs when one infection reduces the transmission of the second pathogen. By contrast, in our study system, we did not see a reduced transmission rate for bTB or brucellosis during coinfection. Individuals infected with bTB were associated with a higher rate of acquiring brucellosis in at least one of our sites but appeared to have no effect in the other site. Brucellosis appeared to have no effect on the transmission of bTB (Fig. 2). Because coinfection was associated with elevated mortality, coinfected individuals were also removed from the population at a faster rate. Competition, therefore, occurs at the population level: bTB is predicted to have a lower prevalence and lower R_0^T in populations where brucellosis occurs compared with populations without brucellosis.

The model structure in this study is informed by our empirical data. As a result, it incorporates realistic age-specific transmission and mortality rates as well as data-driven estimates of the consequences of coinfection. However, additional detail could be added to our model. Specifically, we do not know the consequences of either infection on the other's infection duration or infectiousness, two processes likely to influence persistent infections (18, 22). We also do not consider genetic variation within our buffalo population that may mediate susceptibility to either pathogen. However, our model's ability to accurately represent coinfection patterns with the mechanisms characterized suggests that we have captured the most important processes. Furthermore, our empirical results account for natural variation in demographic and environmental conditions. Thus, our results highlight the importance of coinfection in generating population-level association patterns relative to environmental or genetic drivers of infection.

Given the ubiquity and documented individual-level impacts of chronic coinfections on the host, these results highlight two core challenges in the design and application of integrated control strategies. First, it remains unclear how commonly competition between coinfecting pathogens is occurring. Understanding which pathogens may be competing in coinfected host populations is crucial to estimating the costs and benefits of disease control interventions. For example, in the presence of pathogen competition, removing one pathogen may unintentionally lead to a resurgence of or increases in prevalence of a competing pathogen. Our results suggest that competition at the population level can occur between unrelated pathogens and in the absence of competition for shared resources within the host. Competition appears to be strongest when pathogens have asymmetric effects on transmission. Similar asymmetries in transmission occur in HIV–malaria (6) and HIV–HCV coinfections (33), suggesting a role for this mechanism in other systems.

Second, knowledge on which chronic pathogens are most likely to be influenced by a second infection remains largely theoretical [excluding notable progress with HIV coinfections (6, 22)]. In this study, the immunosuppressive pathogen, bTB (4, 34), was strongly influenced by coinfection at the population level, and our analyses show that bTB prevalence should typically decline in the presence of another chronic pathogen, provided that coinfected hosts suffer greater mortality. This raises the question of whether there are traits of chronic pathogens (e.g., immunosuppressive effects) that make them more likely to be influenced by the presence of other infections. Studies addressing these questions are urgently needed to target both research and treatment on the pathogens most likely to be influenced by coinfection.

Materials and Methods

Model Development. We developed an age-structured, continuous-time disease-dynamic model to explore the consequences of coinfection on bTB and brucellosis infection (Fig. 1). Animals were classified in six groups: susceptible to both infections (S), infected with bTB only (I_T), infected with brucellosis only (I_B), coinfected with both pathogens (I_C), persistently infected with brucellosis but no longer infectious (R_B), or persistently infected with brucellosis but no longer infectious and coinfected with bTB (R_C). We modeled bTB as a lifelong infection with density-dependent transmission (35). Both singly infected (I_T) and coinfected (I_C, R_C) buffalo contribute to bTB transmission. Transmission of brucellosis was assumed to be frequency dependent following modeling work in American bison supporting this assumption (36, 37). Across host species, transmission occurs through ingestion of the bacteria shed in association with aborted fetuses, reproductive tissues, or discharges during birthing [cattle (38), elk (39), and bison (40)]. Singly infected (I_B) and coinfected (I_C) buffalo contribute to brucellosis transmission. Persistently infected buffalo (R_B, R_C) do not contribute to brucellosis transmission, but they do test positive for brucellosis infection. We did not consider vertical transmission because serological evidence suggests that it is rare in African buffalo (41) and experimental evidence for vertical transmission varies by host species [e.g., elk (39)]. Buffalo populations experience density-dependent recruitment, which we modeled with a generalized Beverton–Holt equation (42). This two-parameter representation of density dependence gives a stable age structure and relatively constant population size (ref. 43 and *SI Appendix*, section 2, Fig. S3). A full description of the model is provided in *SI Appendix*, section 2.

The individual-level consequences of coinfection can be summarized by four individual-level processes: (*i*) the effects of prior infection with brucellosis on the rate individuals acquire bTB infection, (*ii*) the effects of prior infection with bTB on the rate individuals acquire brucellosis infection, (*iii*) the effects of coinfection on the per capita mortality rate, and (*iv*) the effects of coinfection on the per capita birth rate. To investigate the consequences of these four individual-level processes on disease dynamics, we quantified the median values of these rates in susceptible, singly infected, and coinfected buffalo. Transmission rates, mortality rates, and the proportional reductions in fecundity with infection are allowed to be age dependent, but recovery and recrudescence are assumed to be independent of age.

Individual-Level Data and Parameter Estimation. We conducted a longitudinal study of 151 female buffalo to estimate the consequences of bTB and brucellosis infection. Buffalo were captured at two locations in the southeastern section of Kruger National Park, radio collared for reidentification, and recaptured biannually at ∼6-mo intervals until June–October 2012. During each capture, we recorded brucellosis infection status, bTB infection status, age, and the animals' reproductive status. Brucellosis testing was conducted with an ELISA antibody test and bTB testing was conducted with a gamma-IFN assay (44, 45). Detailed methodological descriptions of our capture and disease testing protocols are provided in *SI Appendix*, section 3. Animal protocols for this study were approved by the University of Georgia (UGA) and Oregon State University (OSU) Institutional Animal Care and Use Committees (UGA AUP A2010 10-190-Y3-A5 and OSU AUP 3822 and 4325).

We assessed the effects of coinfection on median mortality rates and the median rate at which animals acquired infection by analyzing our longitudinal time-to-event data using semiparametric Cox models where an individual's covariates representing infection change over time. Specifically, we fitted three regression models to predict three events: the time to mortality in uninfected, bTB+, brucellosis+, and coinfected individuals; the time to infection with brucellosis in buffalo with and without bTB; and the time to infection with bTB in buffalo with and without brucellosis. In all analyses, we included age and initial capture site as time-independent, categorical variables and infection status as a time-dependent explanatory variable. We also evaluated whether the association between brucellosis and bTB varied by age or site by including interactions terms between bTB and each environmental variable.

Model Evaluation and Inference. Parameter values for the transmission rate of bTB and brucellosis were estimated by fitting the model to the overall prevalence estimate for bTB and brucellosis in the study population. Our data do not represent a random sample because buffalo aged over the course of the study, with a median age of 3.4 y in buffalo initially captured in June–October 2008. We therefore calculated the overall prevalence for each pathogen after randomly sampling one time point for each buffalo. We estimated the overall prevalence in the study population as the median prevalence in 1,000 replicate samples. We use the prevalence calculated for all buffalo in this study regardless of their initial capture location because prevalence was similar at both locations, herds move and mix within and between sites, and site-specific parameters did not change the qualitative conclusion of this work (*SI Appendix*, section 2, Fig. S9). Model estimates of prevalence were calculated numerically using the deSolve package (46). We calculated prevalence in the model after it had reached equilibrium by representing bTB prevalence as $\pi_T = (I_T + I_C + R_C)/(S + I_T + I_C + R_C + I_B + R_B)$ and brucellosis prevalence as $\pi_B = (I_B + R_B + I_C + R_C)/(S + I_T + I_C + R_C + I_B + R_B)$. The transmission rates of both pathogens were estimated by numerically minimizing the sum of squared differences between the prevalence estimates for bTB and brucellosis in the data and in age-matched estimates of prevalence from the model. We used the Nelder–Mead algorithm implemented with the optim function in R to minimize this function. We evaluated our model by comparing its ability to recreate coinfection patterns in the data, as only the overall prevalence of both pathogens was used for fitting (Fig. 1). We calculated R_0 numerically using the next-generation method (47).

ACKNOWLEDGMENTS. We thank South African National Parks (SANParks) for their permission to conduct this study in Kruger. We thank P. Buss, M. Hofmeyr, and the entire SANParks Veterinary Wildlife Services Department. We thank M. Schrama and the Webb laboratory group for comments on the manuscript and technical support. This study was supported by National Science Foundation (NSF) Ecology of Infectious Diseases Grants EF-0723918/DEB-1102493 and EF-0723928 (to A.E.J. and V.O.E.), NSF Graduate Research Fellowship Program and NSF Doctoral Dissertation Improvement Grant DEB-121094 (to E.E.G.), and Netherlands Organization for Scientific Research (NWO) - Vici Grant 016.140.616 (to R.S.E.).

1. Griffiths EC, Pedersen AB, Fenton A, Petchey OL (2011) The nature and consequences of coinfection in humans. *J Infect* 63:200–206.
2. Gandhi NR, et al. (2006) Extensively drug-resistant tuberculosis as a cause of death in patients co-infected with tuberculosis and HIV in a rural area of South Africa. *Lancet* 368:1575–1580.
3. Alter MJ (2006) Epidemiology of viral hepatitis and HIV co-infection. *J Hepatol* 44:S6–S9.
4. Beechler BR, et al. (2015) Enemies and turncoats: Bovine tuberculosis exposes pathogenic potential of Rift Valley fever virus in a common host, African buffalo. *Proc R Soc Lond B Biol Sci* 282:20142942.
5. Graham AL, Lamb TJ, Read AF, Allen JE (2005) Malaria-filaria coinfection in mice makes malarial disease more severe unless filarial infection achieves patency. *J Infect Dis* 191:410–421.
6. Abu-Raddad LJ, Patnaik P, Kublin JG (2006) Dual infection with HIV and malaria fuels the spread of both diseases in sub-Saharan Africa. *Science* 314:1603–1606.
7. Ezenwa VO, Jolles AE (2015) Opposite effects of anthelmintic treatment on microbial infection at individual versus population scales. *Science* 347:175–177.
8. Abdool Karim SS, et al. (2011) Integration of antiretroviral therapy with tuberculosis treatment. *N Engl J Med* 365:1492–1501.
9. Hotez PJ, et al. (2006) Incorporating a rapid-impact package for neglected tropical diseases with programs for HIV/AIDS, tuberculosis, and malaria. *PLoS Med* 3:e102.
10. Viney ME, Graham AL (2013) Patterns and processes in parasite co-infection. *Advances in Parasitology*, ed Rollinson D (Academic, Oxford), Vol 82, pp 321–369.
11. Lello J, et al. (2013) The relative contribution of co-infection to focal infection risk in children. *Proc R Soc Lond B Biol Sci* 280:20122813.
12. Telfer S, et al. (2010) Species interactions in a parasite community drive infection risk in a wildlife population. *Science* 330:243–246.
13. Pedersen AB, Greives TJ (2008) The interaction of parasites and resources cause crashes in a wild mouse population. *J Anim Ecol* 77:370–377.
14. Martcheva M, Pilyugin SS (2006) The role of coinfection in multidisease dynamics. *SIAM J Appl Math* 66:843–872.

15. Vasco DA, Wearing HJ, Rohani P (2007) Tracking the dynamics of pathogen interactions: Modeling ecological and immune-mediated processes in a two-pathogen single-host system. *J Theor Biol* 245:9–25.
16. Abu-Raddad LJ, Ferguson NM (2004) The impact of cross-immunity, mutation and stochastic extinction on pathogen diversity. *Proc R Soc Lond B Biol Sci* 271:2431–2438.
17. Cummings DAT, Schwartz IB, Billings L, Shaw LB, Burke DS (2005) Dynamic effects of antibody-dependent enhancement on the fitness of viruses. *Proc Natl Acad Sci USA* 102:15259–15264.
18. Huang Y, Rohani P (2005) The dynamical implications of disease interference: Correlations and coexistence. *Theor Popul Biol* 68:205–215.
19. Huang Y, Rohani P (2006) Age-structured effects and disease interference in childhood infections. *Proc R Soc Lond B Biol Sci* 273:1229–1237.
20. Rohani P, Earn DJ, Finkenstädt B, Grenfell BT (1998) Population dynamic interference among childhood diseases. *Proc R Soc Lond B Biol Sci* 265:2033–2041.
21. Rohani P, Green CJ, Mantilla-Beniers NB, Grenfell BT (2003) Ecological interference between fatal diseases. *Nature* 422:885–888.
22. Lloyd-Smith JO, Poss M, Grenfell BT (2008) HIV-1/parasite co-infection and the emergence of new parasite strains. *Parasitology* 135:795–806.
23. Gomo C, de Garine-Wichatitsky M, Caron A, Pfukenyi DM (2012) Survey of brucellosis at the wildlife-livestock interface on the Zimbabwean side of the Great Limpopo Transfrontier Conservation Area. *Trop Anim Health Prod* 44:77–85.
24. Michel AL, Mueller B, van Helden PD (2010) Mycobacterium bovis at the animal-human interface: A problem, or not? *Vet Microbiol* 140:371–381.
25. Waters W, et al. (2011) Tuberculosis immunity: Opportunities from studies with cattle. *Clin Dev Immunol* 2011:768542.
26. Roop RM, Gaines JM, Anderson ES, Caswell CC, Martin DW (2009) Survival of the fittest: How Brucella strains adapt to their intracellular niche in the host. *Med Microbiol Immunol* 198:221–238.
27. Ko J, Splitter GA (2003) Molecular host-pathogen interaction in brucellosis: Current understanding and future approaches to vaccine development for mice and humans. *Clin Microbiol Rev* 16:65–78.
28. Ferguson N, Anderson R, Gupta S (1999) The effect of antibody-dependent enhancement on the transmission dynamics and persistence of multiple-strain pathogens. *Proc Natl Acad Sci USA* 96:790–794.
29. Bhattacharyya S, Gesteland PH, Korgenski K, Bjørnstad ON, Adler FR (2015) Cross-immunity between strains explains the dynamical pattern of paramyxoviruses. *Proc Natl Acad Sci USA* 112:13396–13400.
30. Fenton A (2013) Dances with worms: The ecological and evolutionary impacts of deworming on coinfecting pathogens. *Parasitology* 140:1119–1132.
31. Graham AL (2008) Ecological rules governing helminth-microparasite coinfection. *Proc Natl Acad Sci USA* 105:566–570.
32. Randall J, Cable J, Guschina IA, Harwood JL, Lello J (2013) Endemic infection reduces transmission potential of an epidemic parasite during co-infection. *Proc R Soc Lond B Biol Sci* 280:20131500.
33. Urbanus AT, et al. (2009) Hepatitis C virus infections among HIV-infected men who have sex with men: An expanding epidemic. *AIDS* 23:F1–F7.
34. Beechler BR, Broughton H, Bell A, Ezenwa VO, Jolles AE (2012) Innate immunity in free-ranging African buffalo (Syncerus caffer): Associations with parasite infection and white blood cell counts. *Physiol Biochem Zool* 85:255–264.
35. Jolles AE, Ezenwa VO, Etienne RS, Turner WC, Olff H (2008) Interactions between macroparasites and microparasites drive infection patterns in free-ranging African buffalo. *Ecology* 89:2239–2250.
36. Hobbs NT, et al. (2015) State-space modeling to support management of brucellosis in the Yellowstone bison population. *Ecol Monogr* 85:525–556.
37. Dobson A, Meagher M (1996) The population dynamics of brucellosis in the Yellowstone National Park. *Ecology* 77:1026–1036.
38. Nicoletti P (1980) The epidemiology of bovine brucellosis. *Adv Vet Sci Comp Med* 24:69–98.
39. Thorne E, Morton J, Blunt F, Dawson H (1978) Brucellosis in elk. 2. Clinical effects and means of transmission as determined through artificial infections. *J Wildl Dis* 14:280–291.
40. Rhyan JC, et al. (2009) Pathogenesis and epidemiology of brucellosis in Yellowstone bison: Serologic and culture results from adult females and their progeny. *J Wildl Dis* 45:729–739.
41. Gorsich E, Ezenwa VO, Cross P, Bengis R, Jollesa A (2015) Context-dependent survival, fecundity, and predicted population-level consequences of brucellosis in African buffalo. *J Anim Ecol* 84:999–1009.
42. Getz WM (1996) A hypothesis regarding the abruptness of density dependence and the growth rate of populations. *Ecology* 77:2014–2026.
43. Cross PC, Getz WM (2006) Assessing vaccination as a control strategy in an ongoing epidemic: Bovine tuberculosis in African buffalo. *Ecol Model* 196:494–504.
44. Gorsich E, Bengis R, Ezenwa V, Jolles A (2015) Evaluation of the sensitivity and specificity of an ELISA for diagnosing brucellosis in African buffalo (Syncerus caffer). *J Wildl Dis* 51:9–18.
45. Michel AL, Cooper D, Jooste J, de Klerk LM, Jolles A (2011) Approaches towards optimising the gamma interferon assay for diagnosing Mycobacterium bovis infection in African buffalo (Syncerus caffer). *Prev Vet Med* 98:142–151.
46. Soetaert K, Petzoldt T, Setzer RW (2010) Solving differential equations in R: Package desolve. *J Stat Softw* 33:1–25.
47. van den Driessche P, Watmough J (2002) Reproduction numbers and sub-threshold endemic equilibria for compartmental models of disease transmission. *Math Biosci* 180:29–48.